



UNIVERSITY OF LEEDS

This is a repository copy of *Solar magnetoconvection* .

White Rose Research Online URL for this paper:

<http://eprints.whiterose.ac.uk/990/>

Article:

Hurlburt, N.E., Matthews, P.C. and Rucklidge, A.M. (2000) Solar magnetoconvection. *Solar Physics*, 192 (1-2). pp. 109-118. ISSN 1573-093X

<https://doi.org/10.1023/A:1005239617458>

Reuse

See Attached

Takedown

If you consider content in White Rose Research Online to be in breach of UK law, please notify us by emailing eprints@whiterose.ac.uk including the URL of the record and the reason for the withdrawal request.



eprints@whiterose.ac.uk
<https://eprints.whiterose.ac.uk/>



White Rose
university consortium
Universities of Leeds, Sheffield & York

White Rose Consortium ePrints Repository

<http://eprints.whiterose.ac.uk/>

This is an author produced version of a paper published in **Solar Physics**. This paper has been peer-reviewed but does not include final publisher proof-corrections or journal pagination.

White Rose Repository URL for this paper:
<http://eprints.whiterose.ac.uk/archive/00000990/>

Citation for the published paper

Hurlburt, N.E. and Matthews, P.C. and Rucklidge, A.M. (2000) *Solar magnetoconvection*. *Solar Physics*, 192 (1-2). pp. 109-118.

Citation for this paper

To refer to the repository paper, the following format may be used:

Hurlburt, N.E. and Matthews, P.C. and Rucklidge, A.M. (2000) *Solar magnetoconvection*. Author manuscript available at:
<http://eprints.whiterose.ac.uk/archive/00000990/> [Accessed: *date*].

Published in final edited form as:

Hurlburt, N.E. and Matthews, P.C. and Rucklidge, A.M. (2000) *Solar magnetoconvection*. *Solar Physics*, 192 (1-2). pp. 109-118.

Solar Magnetoconvection

N. E. Hurlburt

*Lockheed Martin Solar and Astrophysics Laboratory, Organization L9-41 Building
252, Palo Alto, CA 94304, USA*

P. C. Matthews

*School of Mathematical Sciences, University of Nottingham, University Park,
Nottingham NG7 2RD, UK*

A. M. Rucklidge

*Department of Applied Mathematics and Theoretical Physics, University of
Cambridge, Cambridge, UK CB3 9EW*

Abstract. In recent years the study of how magnetic fields interact with thermal convection in the Sun has made significant advances. These are largely due to the rapidly increasing computer power and its application to more physically relevant parameters regimes and to more realistic physics and geometry in numerical models. Here we present a survey of recent results following one line of investigations and discuss and compare the results of these with observed phenomena.

Keywords: convection – hydromagnetics – stars; interiors – Sun: magnetic fields

1. Introduction

Our physical understanding of solar magnetoconvection has made great strides in recent years as a direct result of the new generation of large-scale computers. The increase in memory and speed permit researchers to investigate computational domains with greater resolution, over a larger physical scale, and in three dimensions. We can divide the various strains of recent investigations into two classes: those emphasizing bigger computational boxes, and those emphasizing better computational boxes.

Two recent examples of the former class investigate solar magnetoconvection in domains spanning large horizontal scales (much larger than the layer depth). Cattaneo (1999) studied Boussinesq magnetoconvection at high magnetic Reynolds numbers in rectangular domains with aspect ratios of at least 10. He discovered that small, random seed fields were amplified by the turbulent convection present in the simulations. The resulting magnetic field maintained a net flux of zero, but had large rms field strengths in the interstices between convection cells. The resulting magnetic field distribution looked surprisingly similar to that observed in magnetograms obtained by the MDI instrument on SOHO.



© 1999 Kluwer Academic Publishers. Printed in the Netherlands.

Meanwhile Tao et al. (1998), in a study of large-scale compressible magnetoconvection, discovered regimes of multiscale magnetoconvection. In regions of moderate magnetic flux, large-scale convection cells sweep most of the magnetic flux into the cell boundaries – as has been observed in all magnetoconvection experiments since Weiss (1966). However, unlike previous, small-box results, the fields did not attain strengths sufficient to suppress convection within them. Instead a patchwork of field-free, large-scale convection and strong-field, small-scale convection formed. Again this is consistent with observations of active regions, where the plage regions typical display anomalous convection on granular scales, interspersed with normal, quiet-sun granulation (Title et al., 1992).

Here we present a series of results aimed at understanding magnetoconvection within active regions – particularly in the immediate vicinity of sunspots. We follow the alternative path by focusing our computing power on improving the geometry and underlying physics of the problem to better reflect the observed dynamics. We find that many of the observed properties of magnetoconvection around sunspots are captured by these relatively simple models, including umbral dots and penumbra grains, fluted sunspot penumbra and the Evershed flow, sunspots moats and sources for coronal heating.

In the next section we present the basic properties shared by all the various models we discuss. This is followed by a presentation of how the various models mimic observed phenomena. We conclude with a discussion of the overall relevance to solar observations and what we may see in the near future.

2. The Basic Model

All the simulations we present share the same basic physical model. (See Hurlburt and Rucklidge (1999) for the most recent description.) We consider a plane-parallel layer of gas experiencing a uniform gravitational acceleration in the vertical (z) direction. This perfect, monatomic gas has constant dynamic viscosity, resistivity, and thermal diffusivity, as well as a constant ratio of specific heats, $\gamma = 5/3$. The horizontal surfaces containing this layer are impenetrable and stress-free.

The stratification in the absence of motion is simply that of a polytrope, where temperature, density and pressure have the form

$$T_s = 1 + \theta z, \quad \rho_s = (1 + \theta z)^m, \quad P_s = (1 + \theta z)^{m+1}, \quad (1)$$

where the polytropic index m measures the gravitational acceleration and θ is an integration constant which represents the dimensionless temperature gradient across the layer.

The degree of instability may be measured by the Rayleigh number, which has a local value of

$$R = \theta^2(m+1)(1 - (m+1)(\gamma-1)/\gamma) \frac{(1+\theta z)^{2m-1}}{\sigma K^2}, \quad (2)$$

where K is the dimensionless thermal conductivity and σ is the Prandtl number. Since R varies with depth, it is most convenient to evaluate it at midlayer, thereby setting $R(z_0 + \frac{1}{2}) \equiv R_a$.

The effect of the magnetic field upon the convective stability can be measured by the Chandrasekhar number Q which is related to the usual ‘plasma beta’ β at the mid-point of the layer by

$$\beta = \frac{2(1+\theta/2)^{(m+1)}}{Q\zeta_0\sigma K^2}. \quad (3)$$

The magnetic Prandtl number is proportional to density $\zeta = \zeta_0\rho_s$ and hence increases monotonically with depth. In what follows, all simulations are conducted with $\theta = 10$, $\sigma = 1.0$, $\zeta_0 = 0.2$ and $m = 1.0$. The Rayleigh is in the range $R_a \approx 100,000$ while the Chandrasekhar number varies, depending upon the choice of boundary conditions, geometry, etc.

We have used two distinct numerical methods. Calculations in Cartesian geometry are carried out using a hybrid pseudo-spectral/finite-difference technique for spatial derivatives and an Adam-Bashforth time-stepping scheme. (See Hurlburt et al. (1996) and Matthews et al. (1995) for details.) Calculations in cylindrical geometry are conducted using a sixth-order compact difference scheme for spatial derivatives and a modified Bulirsch-Stoer method for advancing the solutions in time. (See Hurlburt and Rucklidge (1999) for details.)

3. Results

3.1. IN THE UMBRA

In the dark umbra of a spot, the field is relatively uniform and very close to vertical. In such circumstances models using simple, vertical field boundary conditions or ones that match the boundary field to a uniform potential field are appropriate, as is the use of Cartesian geometry with periodic boundary conditions on the sides. The configuration with vertical fields has been explored by Hurlburt and Toomre (1988) and Weiss

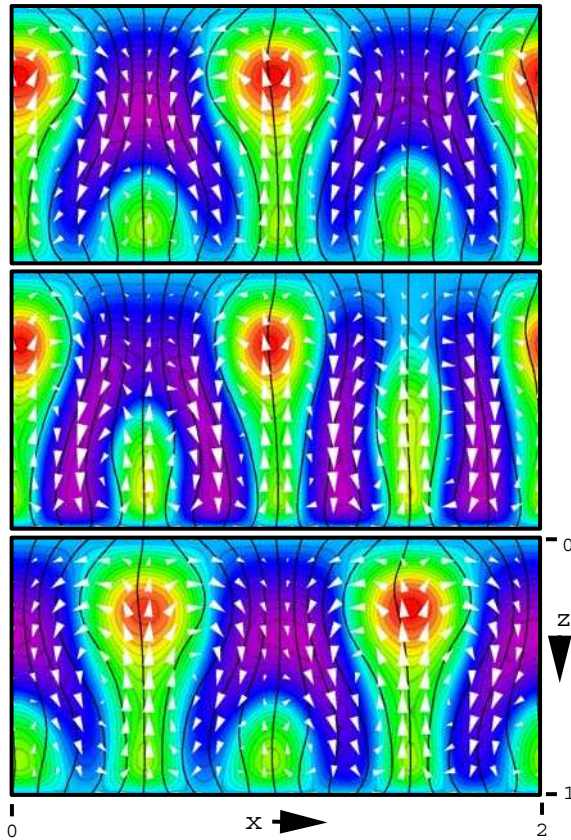


Figure 1. Features that resemble umbral dots in uniform, vertical fields carry heat from beneath into the low β plasma in the umbra. Here a solution with $R_a = 80,000$ and $Q = 1000$ is displayed at three times. (From HMP.) The arrows indicate the velocity of the fluid, the black lines are magnetic field lines and the background grey scale displays the temperature fluctuations relative to the initial state.

et al. (1990) in two dimensions and more recently by Matthews et al. (1995) in three dimensions; Hurlburt et al. (1996) (hereafter referred to as HMP) and Blanchflower et al. (1998) have investigated the potential field case in two dimensions. Here we present results following these later studies, but in three dimensions.

In all cases, a behavior similar to that displayed in Figure 1 is found. Relatively steady, small convection cells form in the region where the magnetic Prandtl number ζ exceeds unity. In the sun this occurs at depths between 10 and 20 Mm. The upward plumes within adjacent cells alternately rise in to the upper portions of the layer where ζ is less than unity and $\beta \approx 1$, and where linear stability leads us to expect the complete suppression of convection. The plumes thereby couple the

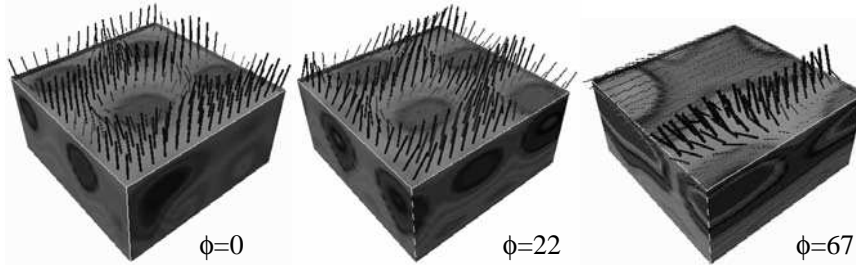


Figure 2. Features that resemble umbral dots in uniform, vertical fields, become traveling waves in slightly-inclined fields, and give way to roll-like solutions for highly-inclined fields. In these three-dimensional simulations, $R_a = 64,000$ and $Q = 1333$. The temperature is displayed as a grey scale (with hot material darker) on the sides and near the surface of the computational domain. The small cylinders represent the direction and strength of the magnetic field at the surface.

two regions and bring heat into the upper portions of the umbra. In three dimensions the convection forms a lattice of dots, as seen in Figure 2a, which pulsate in a similar manner. Weiss et al. (1990) conjectured this is the cause of the small umbral dots observed in sunspot umbra. They estimated the lifetimes of these dots to be on the order of hours, much longer than the characteristic Alfvén time.

3.2. IN THE PENUMBRA

In the outer portions of the umbra and penumbra, the approximations that the field is vertical and uniform field are inappropriate. To investigate the behavior of magnetocovection in these circumstances we turn to Cartesian models with inclined fields for investigating small-scale (relative to the sunspot radius) motions and to cylindrical models for larger scale motions.

The inclined field can most easily be imposed by using potential field boundary conditions with the requirement that the field be uniformly inclined at an angle ϕ from the vertical at large distances from the computational domain. HMP considered the problem in two dimensions and found a preference for traveling wave solutions. In figures 2 and 3 we present the three-dimensional equivalent of their results for different inclinations. When the field is inclined only slightly (figures 2b and 3a), the cellular structure of the flows appears similar to the umbral dot model in Figure 2a. However the dots no longer pulsate in a stationary lattice. Instead they travel with a fixed velocity away from the direction of tilt (leftwards in figure 2b and downwards in figure 3). HMP found that the speed of the pattern in their two-dimensional model was proportional to the inclination, so these dots would slow down as they approached the umbra.

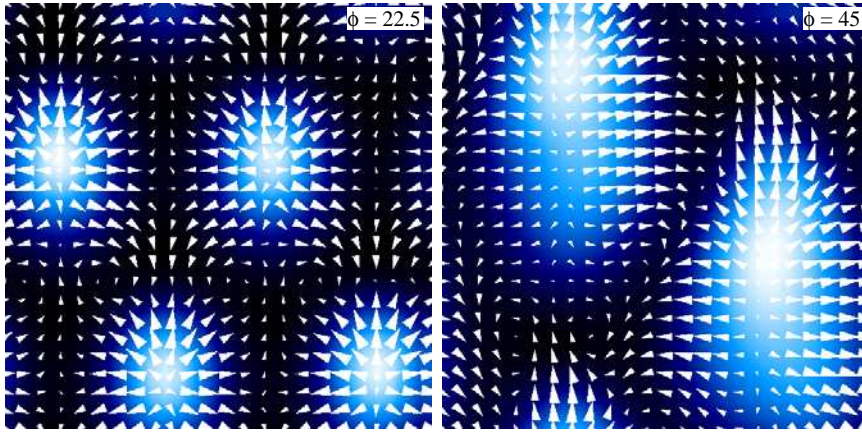


Figure 3. The temperature and surface velocity of three dimensional solutions with mean field inclinations of $\phi = 22.5$ deg and $\phi = 45$ deg. The grey scale denotes the temperature of the fluid near the upper boundary and the small triangles denote the velocity of the surface flow (with area proportional to speed).

This behavior is similar to what is seen in penumbra grains and moving umbral dots. High resolution observations reveal that there appears to be a steady inflow of these grains in the periphery of the umbra and immediately outside of it. In our model the motion is a pattern or wave moving through the spot, and is not associated with a net flow of material or field. In fact if one considers what would be the Doppler signal from these cells it is clear that there is an apparent mean flow outwards due to the asymmetries of the flows around the hot plumes.

As the inclination increases the scale of the cells increases in the direction of inclination. For inclinations of 45 degrees (figure 3b), the cells are twice the size of those in the vertical case, and the asymmetry in the surface flow surrounding the hotter material is even more evident. As the cell moves through the field towards the center of the spot, it leaves behind a wake of rapidly moving fluid moving outwards, and a small circulating flow around it. This signature – cellular patterns moving inwards against and apparent outflow – offers an explanation for the observed behavior in sunspot penumbra.

As the field becomes more nearly horizontal (figure 2c), the cell structure gives way to more roll-like solutions. The magnetic field is concentrated into the dark lanes and the flow within these lanes moves uniformly outwards. The brighter regions show a stronger and more complex cellular structure.

Thus much of the structure and dynamics observed on the small scale within sunspots appears to be captured by our simple model – once

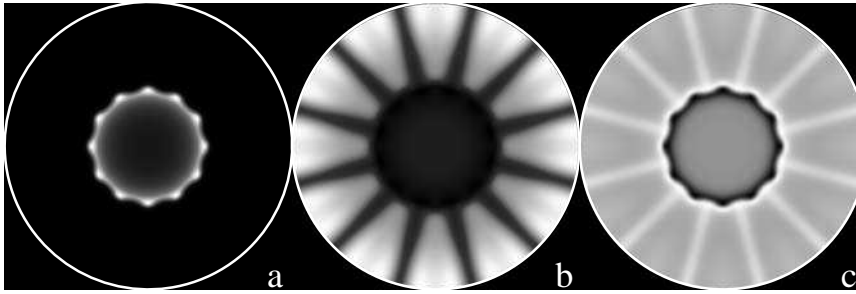


Figure 4. The surface structure of a cylindrical solution forms striations similar to sunspot penumbra. Here we display the (a) vertical magnetic field, (b) temperature and (c) density for a steady solution with $R_a = 100,000$ and $Q = 64$.

we include appropriate field geometry. On larger scales, the roughly cylindrical shape of a sunspot or pore must also be taken into account. The simplest means for doing this is to consider axisymmetric models, which we will do in the following section. We first present some recent results of a three-dimensional cylindrical model which casts light on the formation and structure of sunspot penumbra.

Figure 4 displays the vertical magnetic field, temperature and density near the upper boundary of a simulation in a cylindrical geometry. In this case the computational domain consists of a wedge spanning $\pi/6$ radians with periodic boundary conditions in azimuth. The outer boundary is impenetrable, stress-free, thermally insulating and perfectly conducting; the upper and lower boundaries are held at a fixed temperature with vertical magnetic field. The steady state for this case consists of an isolated flux tube centered on the axis, as seen in the magnetic field Figure 4(a). The field strength is uniform in the center of the tube, and displays a maximum on its periphery. This periphery has an azimuthal structure, forming localized points of peak field strength. The temperature and density within the tube drops to about 80% and 40% of the surroundings respectively, and reach their minimums of about 70% and 20% just within the edge of the flux tube. The convection outside of the tube arranges itself into cells which are elongated in the radial direction, forming a structure that looks like a rudimentary penumbra. The fluid at the boundaries of these cells is both cooler and denser than average. It seems that this pattern is preferred over the purely axisymmetric models studied by Hurlburt and Rucklidge (1999) since we have been unable to produce axisymmetric solutions which are stable to non-axisymmetric perturbations in these three dimensional models. Hence the formation of penumbra may well be a natural consequence the cylindrical cross section of a flux tube.

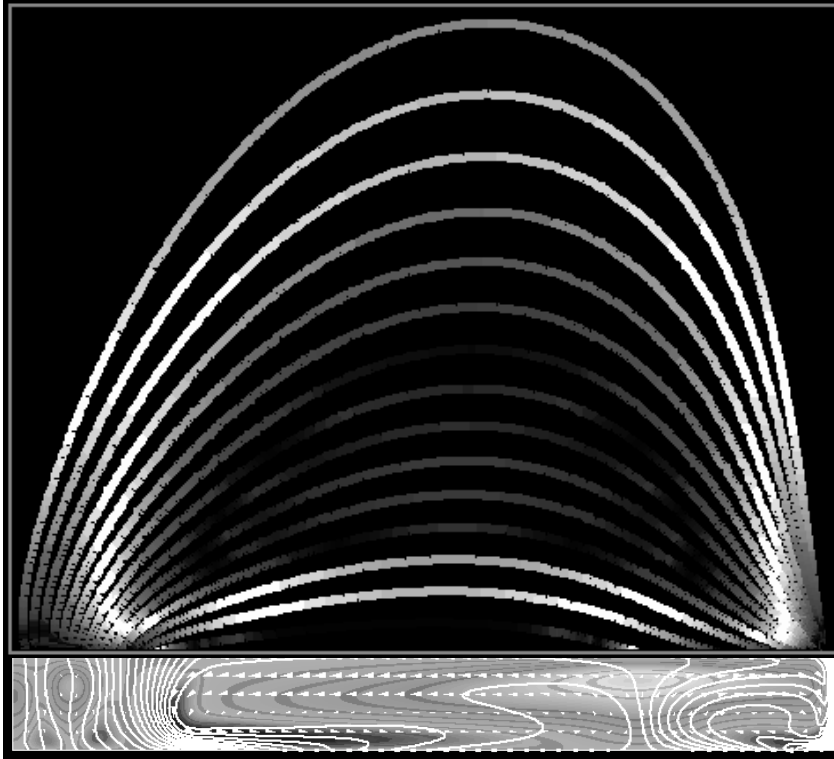


Figure 5. Formation and heating of coronal loops using coupled magnetoconvection model, potential field and coronal heating model. Here $R_a = 100,000$ and $Q = 300$.

3.3. ABOVE AND BELOW SUNSPOTS

On the largest scale, we must consider not only the flows in the immediate vicinity of sunspots, but also those corresponding to the returning magnetic field. To begin to address this situation we consider large-aspect ratio, axisymmetric models which include the return flux. This model is based upon the axisymmetric code developed by Hurlburt and Rucklidge (1999). The boundary conditions at the upper surface is radiatively cooled using Stefan's Law and the magnetic field is potential, vanishing at infinity. The temperature and field lines are fixed at the lower boundary. Figure 5 displays one such calculation with an aspect ratio of 9. The magnetic field is concentrated into the center by a very large cell which is flowing toward the center at the surface. As found by Hurlburt and Rucklidge (1999) all our axisymmetric solutions relax to such a state. The field within this concentration does not

completely suppress the smaller-scale, umbral dots (or umbral rings in this case), and these tend to migrate inwards slowly. At the outer edge of the domain, a moderate-scale cell forms which confines most of the returning magnetic flux to a narrow layer at the outer boundary.

The potential field overlying the computational domain is also shown. Note that the field lines show a wide range of inclinations at the surface and that there is a significant difference in the local flow associated with each field line as it departs the computational domain. Both these factors result in a spatially-varying Poynting flux ($\mathbf{E} \times \mathbf{B}$) of energy into the outer layer.

The brightness of the loops in figure 5 displays a first attempt to explore how such motions would heat the loops in the corona (Alexander et al., 1999). These lines and the associated Poynting fluxes from the solution were used as inputs into a simple RTV heating model (Rosner et al., 1978). The magnitudes of the velocity and magnetic field were scaled to typical sunspot values and the resulting EUV emission was passed through the TRACE 171A response function to obtain the relative visibility of the various loops. It is clear from the figure that both loops high and low in our idealized corona show significant brightening. The higher loops are heated by the motions of the moving penumbral grains on the periphery of our model spot, while the low loops are heated by the strong cross-field flows which maintain the boundary of the spot.

4. Conclusions

We have presented a series of related numerical models which offer insight into the dynamics of magnetoconvection in sunspots and their surroundings. We find the key elements to much of the observed behavior within sunspots appears to be due to purely geometric effects.

On the largest scale, the formation and maintenance of sunspots appears to be controlled by the large scale convection cell flowing inward at the surface. The axisymmetric calculations of Hurlburt and Rucklidge (1999) suggest that this is the basic mechanism and conjectured that the apparent disagreement with observations of moat flow around sunspots is due to the inflowing “collar” residing beneath the observed penumbra. The convection in the vicinity of the resulting, roughly-cylindrical flux tube is then prone to form radial striations as the non-axisymmetric modes develop, forming spines and flutes in the magnetic field configuration on the large scale.

Within the region of strong field, large-scale convection is suppressed and replaced by smaller-scale cells. These cells exist within a magnetic

field that is generally inclined to vertical. In the umbra, where the field is nearly vertical, the convection arranges itself to form tall, narrow cells, or umbra dots which pulsate near the surface, heating the umbra. In the outer umbra and inner penumbra, where the fields become significantly inclined, these cells become moving umbral dots and penumbra grains which travel inwards with speeds proportional to the inclination. These inclined cells are accompanied by mean shear flows, which manifest themselves as the outward Evershed flow. The magnetic field lines in the corona which are connected to these moving dots and grains can be heated by the resulting Poynting flux as proposed by Martens et al. (1996) and form the coronal feature known as X-ray anemone.

In the outer reaches of the penumbra, the high inclination of the field causes a scale change and the transition from tall, narrow convection cells to convective rolls aligned in the direction of tilt. As this transition occurs the field becomes concentrated into strong, vertical flutes in the dark, cooler regions, as observed by Title et al. (1993) and Lites et al. (1993).

While suggestive, the behavior of the models presented here remain far from realistic. To move them beyond mere mimicry, we must include more of the key features that we expect to find in solar convection zone, such as higher Reynolds numbers, improved treatments of radiation and ionization, and transmitting boundary conditions. However, the simplicity of our models and their surprising agreement with observation suggest that many of the key features responsible for the structure and dynamics within sunspots may have already been captured.

Acknowledgements

We wish to thank D. Alexander, N. Weiss, M. Proctor, F. Cattaneo, A. Title, R. Shine and T. Tarbell for their insights and observations. This work was supported by NASA through grant NAG5-7376 at Lockheed Martin and grant NAG5-3077 at Lockheed Martin and Stanford. AMR is grateful for support from the Royal Astronomical Society.

References

- Alexander, D., N. E. Hurlburt, and A. M. Rucklidge: 1999, 'Heating the atmosphere above sunspots'. *submitted Solar Phys.*
- Blanchflower, S. M., A. M. Rucklidge, and N. O. Weiss: 1998, 'Modelling photospheric magnetoconvection'. *Mon. Not. Roy. Soc.* **301**, 593–608.
- Cattaneo, F.: 1999, 'On the Origin of Magnetic Fields in the Quiet Photosphere'. *Astrophys. J.* **515**, L39–L42.

- Hurlburt, N. E., P. C. Matthews, and M. R. E. Proctor: 1996, 'Nonlinear Compressible Convection in Oblique Magnetic Fields'. *Astrophys. J.* **457**, 933+.
- Hurlburt, N. E. and A. M. Rucklidge: 1999, 'Development of structure in pores and sunspots: flows around axisymmetric magnetic flux tubes'. *submitted Mon. Not. Roy. Soc.*.
- Hurlburt, N. E. and J. Toomre: 1988, 'Magnetic fields interacting with nonlinear compressible convection'. *Astrophys. J.* **327**, 920–932.
- Lites, B. W., D. F. Elmore, P. Seagraves, and A. P. Skumanich: 1993, 'Stokes Profile Analysis and Vector Magnetic Fields. VI. Fine Scale Structure of a Sunspot'. *Astrophys. J.* **418**, 928+.
- Martens, P. C., N. E. Hurlburt, A. M. Title, and L. W. Acton: 1996, 'An Analytical Model for Fluted Sunspots and a New Interpretation of Evershed Flow and X-Ray Anemones'. *Astrophys. J.* **463**, 372+.
- Matthews, P. C., M. R. E. Proctor, and N. O. Weiss: 1995, 'Compressible magnetoconvection in three dimensions: planforms and nonlinear behaviour'. *J. Fluid Mech.* **305**, 281–305.
- Rosner, R., W. H. Tucker, and G. S. Vaiana: 1978, 'Dynamics of the quiescent solar corona'. *Astrophys. J.* **220**, 643–645.
- Tao, L., N. O. Weiss, D. P. Brownjohn, and M. R. E. Proctor: 1998, 'Flux Separation in Stellar Magnetoconvection'. *Astrophys. J.* **496**, L39+.
- Title, A. M., Z. A. Frank, R. A. Shine, T. D. Tarbell, K. P. Topka, G. Scharmer, and W. Schmidt: 1993, 'On the magnetic and velocity field geometry of simple sunspots'. *Astrophys. J.* **403**, 780–796.
- Title, A. M., K. P. Topka, T. D. Tarbell, W. Schmidt, C. Balke, and G. Scharmer: 1992, 'On the differences between plage and quiet sun in the solar photosphere'. *Astrophys. J.* **393**, 782–794.
- Weiss, N. O.: 1966, 'The expulsion of magnetic flux by eddies'. *Proc. A. Roy. Soc.* **293**, 310–328.
- Weiss, N. O., D. P. Brownjohn, N. E. Hurlburt, and M. R. E. Proctor: 1990, 'Oscillatory convection in sunspot umbrae'. *Mon. Not. Roy. Soc.* **245**, 434–452.

